

Quantum Enhanced Deep Learning Bio Inspired Model for Lung Tumors Detection and Severity Analysis in Clinical CT-DICOM Images

Kalaivani Devaraj^{1,2*} and Dheepa Ganapathy¹

¹Department of Computer Science, PKR Arts College for Women, Tamilnadu, India.

²Department of Computer Science, PPG College of Arts and Science, Tamilnadu, India.

<http://dx.doi.org/10.13005/bbra/3435>

(Received: 29 May 2025; accepted: 12 July 2025)

To propose a hybrid quantum-based deep learning model to detect malignant lung nodules and accurately classify disease severity. Bio-inspired techniques are integrated to optimize the learning rate for robust generalization. A Hybrid Quantum-Enhanced Deep Neural Network (QE-DNN) combined with a Quantum Convolutional Neural Network (Q-CNN) is used to extract the multi-scale spatial patterns from high-resolution CT-DICOM images. To perform deep segmentation, Quantum Mask-RCNN is used to isolate the ROI from the images effectively. A bio-inspired Adaptive Firefly-Differential Evolution (AFDE) optimizer is employed to fine-tune the learning architecture. Quantum histogram equalization and wavelet fusion are incorporated as data pre-processing methods to retain critical edge and intrinsic features. CT-DICOM dataset is used for evaluation which consists of 25,1135 images with a resolution of 512x512 pixels. The performance is assessed in MATLAB, TensorFlow Quantum, and IBM Qiskit tools by comparing the proposed work with existing models such as SVM-WSS, GCPSO-PNN, 3D-DLCCNN, and ECNNDE-BCE. The proposed QEDNN-AFDE quantum bio-inspired nodule detection strategy enhanced the generalization capability by exploring wider with proven results of 96.4% accuracy, 95.2% sensitivity, 95.8% specificity, 95.2% F1 score, 94.6% dice coefficient, 0.02 Log Loss and AUC-ROC with 0.95 TPR and 0.05 FNR. The proposed QEDNN-AFDE model strengthens the interpretability of deep learning models in medical imaging and sets a new benchmark in quantum-assisted diagnostics in precision oncology. The model shows promising performance in both classification accuracy and severity prediction and outperforms all existing models.

Keywords: Classification; Data Processing, Image Segmentation; Lung Nodules Detection; Mask R-CNN; Quantum Convolutional Neural Network.

Lung cancer is one of the most fatal malignancies, and it is a leading cause of cancer-related deaths globally, often diagnosed at advanced stages. The severity of lung cancer ranges from localized to aggressive metastatic tumors. Early detection with accurate severity grading is crucial for better treatment strategies, prognosis, and survival outcomes in non-small and small-cell

lung cancers. As we are in AI and medical imaging technological advancements, deep learning methods have shown high potential in early-stage automated tumor detection and classification by extracting multiple features. However, the prevailing techniques can detect tumors but often struggle with feature ambiguity, poor generalization, and suboptimal segmentation in heterogeneous clinical

*Corresponding author E-mail: kalairathin@gmail.com



datasets. To address the limitations of prevailing models, this research proposes a hybrid deep learning quantum framework using a Quantum-Enhanced Deep Neural Network with Adaptive Firefly-Differential Evolution (QEDNN-AFDE) to detect and classify lung tumors and severity analysis with high accuracy. This approach's uniqueness lies in quantum-inspired amplitude encoding, quantum convolutional layers, and evolutionary optimization to enhance the learning rate and diagnostic precision. The proposed work is compared against SVM-WSS, GCP SO-PNN, 3D-DLCNN, and ECNNDE-BCE models. The key contributions of this study include Novel QEDNN architecture for enhanced spatial representation, AFDE for adaptive hyperparameter tuning, deployment of quantum-enhanced Mask-RCNN for deep segmentation, and quantum pre-processing methods. This research is tailored for real-world clinical integration, which is scalable and high-precision and sets a benchmark for lung cancer diagnostics in the healthcare sector.

A deep CNN model with a dual attention mechanism was proposed to enhance lung nodule detection from CT-MICRO images. The model outperforms with a high sensitivity ratio, detecting subtle nodule patterns in dense regions. However, deep CNN architecture lacks adaptability and generalization in multi-class scenarios for diverse anatomical structures. Also, the study does not include an optimization strategy, limiting diagnostic completeness.¹ Hybrid quantum architecture combined with radiographs and CT images was introduced to detect lung cancer at an early stage. In this model, quantum noise processing is employed to improve the classification accuracy. The model lacks a dedicated segmentation mechanism, which limits the spatial precision in extracting ROI in images. The authors mainly focused on binary classification without addressing the severity grades, which leads to a limited scope beyond boundary diagnosis.² ExtRANFS, an automated malignancy detection mechanism with a random feature selection method, is proposed to improve tumor detection accuracy. However, the model highly depends on handcrafted features, limiting robustness and scalability across diverse patient profiles. End-to-end segmentation is limited in this model as it lacks clinical applicability and interpretability.³ Standard

CNN deep learning model differentiates the cancer stages and severity levels. The CNN layers deeply processed the feature maps and performed based on threshold test runs. This model's limitations lie in ROI localization and hyperparameter tuning, which is crucial for multi-class tasks.⁴ VGG-16 and the traditional CNN model were evaluated for lung cancer detection from CT scans. The model outperforms with 85% classification accuracy, which lacks robust optimization towards deep medical image analysis and region-specific learning capabilities. The absence of pre-processing enhancements affects the model's sensitivity, leading to noise inputs to the segmentation and masking system.⁵ The IWD-ARP bio-inspired optimization model was proposed to demonstrate the utility of water drops in the decision-making process. The concept inspired the adoption of the nature-inspired algorithm in lung cancer prediction to tune the deep hyperparameters, which is central to this proposed research work.⁶ The SVM-WSS classical approach was developed to predict lung cancer using structured datasets. A three-stage approach is followed in the research to attain multi-class objectives. 85% accuracy is achieved by the model, which is unsuitable for critical diagnostic applications. A few limitations noted in this model are the lack of segmentation, adaptability, and optimization, which is crucial for a high-performing multi-class decision support system.⁷

GCP SO-PNN lung cancer segmentation and classification bio-inspired model is introduced to improve the ROI selection and to work on complex datasets. The classification uses CNN layers, incorporating edge selection and a boundary marking strategy. The model's optimization process is completely lacking, leading to inadequate feature learning and faster convergence in real-time applications.⁸ A 3D-DLCNN model with a DICOM dataset was proposed to target three classes and was implemented successfully using spatial and temporal feature extraction. Though the model attained 86% accuracy, it lacks memory constraints and adaptive optimization, limiting scalability and convergence. The data distribution between layers is highly impacted due to its fixed learning parameters.⁹ ECNNDE-BCE¹ was proposed to enhance lung nodule detection and classification. The model uses the BCE loss

function to improve classification and minimize false alarms. The model’s segmentation phase delivers high-precision output, leading to a better decision-making system. The model’s limitation lies only in quantum precision and quantum layer segmentation, which are crucial for high interpretability for clinical use.¹⁰

MATERIALS AND METHODS

The proposed model focused on a novel quantum-based deep learning method integrated with a bio-inspired optimization learning mechanism to detect lung tumors and highly accurately analyze the severity score using CT-DICOM images.

Quantum Enhanced Deep Neural Network (QE-DNN), Quantum Mask-RCNN (QM-RCNN), and Adaptive Firefly-Differential Evolution (AFDE) methods are used for feature analysis, deep segmentation, and hyperparameter tuning and optimization. The proposed framework utilizes quantum-enhanced pre-processing, enabling the model to detect subtle tumor characteristics better. The model aims to enhance diagnostic precision and clinical interpretability using intelligent, quantum-based bio-inspired architecture. Figure 1 shows the flow diagram of the quantum hybrid framework and its methodology.

CT-DICOM Data Description and Partition Strategy

This research study utilizes the CT-DICOM dataset with 251135 images collected from the TCIA repository with tumor presence, severity scores, and bounding boxes annotations. All the images with standard pixel size 512x512 include greyscale combinations. The dataset is partitioned for training, testing, and validation purposes with a ratio of 70:20:10. Table 2 shows the dataset attributes and values with major features used for this research work to meet the objective. The data splitting is done exclusively for training, tuning, and unbiased end assessment.

Quantum-Enhanced Image Pre-Processing using QHE and WEF

In order to enhance the raw data quality and boost the robust feature learning data-preprocessing is required. In this research study, quantum enhanced image processing pipeline is employed to refine the CT-DICOM images prior

to segmentation and classification stage. The pre-processing consists of four stages such as i) intensity normalization ii) histogram equalization iii) wavelet-based noise removal and iv) quantum-based feature transformation.

For intensive normalization, the variability is measured in HU (Hounsfield Units) across every CT-DICOM, the images are normalized to standard intensity ranges. The min-max normalization technique is applied for each image pixel $I_{i,j}$. The normalization equation is expressed in Equation 1.

$$I'_{i,j} = \frac{I_{i,j} - I_{min}}{I_{max} - I_{min}} \quad \dots(1)$$

where, I_{max} , I_{min} represents minimum and maximum HU values in the DICOM input image. This method ensures greater consistency in greyscale representations across datasets which is highly essential for downstream quantum encoding. In order to improve the contrast between the healthy and malignant tissues in DICOM, QHE (Quantum Histogram Equalization) is adopted by using Hadamard-based encoding. Here, image data is mapped into QSV (Quantum State Vector) $|\psi\rangle$, the Equation 2 is expressed as,

$$|\psi\rangle = \sum_{i=0}^{N-1} \alpha_i |i\rangle, \text{ where } \alpha_i = \frac{I'_i}{\sqrt{\sum_k (I'_k)^2}} \quad \dots(2)$$

Where, QHE enhances local and global contrasts and redistributes the intensity levels allows the high visibility of lung tumors while preserving the tissue structure. In the next stage, the high-frequency noise is removed while retaining the anatomical edges, Wavelet Fusion Enhanced (WFE) method is applied. The raw image is I is decomposed into A called quantum approximation. The detailed coefficients D_h , D_v , D_d (Horizontal, Vertical and Diagonal) is mathematically expressed in Equation 3 is as follows.

$$I(x, y) = A(x, y) + D_h(x, y) + D_v(x, y) + D_d(x, y) \quad \dots(3)$$

where, thresholding is performed on three coefficients to remove noise without affecting the nodule borders. The final output I_{clean} will be taken as for denoising and segmentation tasks. After denoising the images, all the features are encoded into QS (Quantum States) for downstream segmentation and classification which is shown in next section. The pixel intensities are represented in superposition state by using the Amplitude Coding method which is expressed in the below Equation 4.

$$|\phi\rangle = \sum_{i=0}^{N-1} \frac{x_i}{\|x\|} |i\rangle, \text{ where } \|x\| = \sqrt{\sum_i x_i^2} \quad \dots(4)$$

where, the transformation process enables QCL (Quantum Convolutional Layers) to operate efficiently to capture spatial relationships which is not evident in classical convolutional layers.

ROI Segmentation using Quantum Mask-RCNN

The accurate and deep segmentation of lung nodules is crucial for detection and classification tasks. To attain high spatial ROI extraction, a novel Quantum Mask Region-Based CNN (QM-RCNN) combines the classical layers into quantum encoding to enhance boundary recognition, especially in low contrast or ambiguous anatomical regions.

The Mask R-CNN deep segmentation tasks are carried out in five different stages such as,

1. Input Preparation and Feature Encoding
2. Region Proposal Network
3. Quantum-Assisted ROI Alignment
4. Segmentation and Masking
5. Output and ROI Extraction

Input Preparation and Feature Encoding

The process begins with the pre-processed CT-DICOM images, which undergo QFT (Quantum Feature Transformation) through the amplitude encoding process. Each image in the pipeline is transformed into HD vector space where each pixel's intensity level highly contributes to the amplitude of quantum states. This dynamic encoded representation captures the subtle differences in density and texture, which

helps discriminate between benign and malignant tumors.

Region Proposal Network (RPN)

RPN predicts bounding boxes for potential nodules. These region proposals are generated based on the anchor boxes with different aspect ratios and scales. Quantum encoding enables the RPN to localize the minute abnormalities accurately, which improves the contrast of faint nodules. The feature maps from this stage serve as input for mask prediction and classification implemented in QEDNN and AFDE frameworks.

Quantum-Assisted ROI Alignment

After the RPN process, each proposed region undergoes ROI alignment, which is enhanced using a quantum-weighted Attention Mechanism. This QWAM technique assigns dynamic weights to each region based on relevance to Q-derived context in order to ensure that nodules with irregular shapes are not misaligned during feature pooling or extraction. The Q-Attention score $Q_{\text{attention}}$ for region r is computed as,

$$Q_{\text{attention}}(r) = \sum_{i=1}^N \alpha_i \cdot f_i(r) \quad \dots(5)$$

where, α_i is Q-derived coefficients and $f_{i(r)}$ is region specific features.

Segmentation and Masking

After the complete process of feature alignment, the aligned features are then passed into quantum-enhanced convolutional decoder which decodes the output as a binary mask for each detected region. Each pixel in the detected mask is assigned a value based on learned spatial patterns which enables the precise boundary detection. The mask loss function L_{mask} is mathematically expressed in Equation 6 as follows.

$$L_{\text{mask}} = -\frac{1}{N} \sum_{i=1}^N [M_i \log(M_i) + (1 - M_i) \log(1 - M_i)] \quad \dots(6)$$

where, M_i and M_i^{\wedge} is ground truth and predicted mask value of the segmentation process.

Output and ROI Extraction

A set of segmented masks corresponding to individual nodules is extracted as the final output

of the QM-RCNN. These masks are fully overlaid on the original DICOM image to extract the ROI patches, and each patch is labeled based on its severity score and passed to the QEDNN classifier for detection and classification. The QM-RCNN segmentation model achieves a Dice Coefficient of 94.6%, which outperforms all existing models in terms of superior boundary conformity and accuracy in anatomical scenarios.

Hybrid QEDNN-AFDE Framework for Tumor Detection and Multi Classification

To overcome the limitations of existing models on precise tumor detection and effective multi-class classification in CT-DICOM images, a hybrid framework is proposed in this research work by integrating Quantum-Enhanced DNN with Adaptive Firefly Differential Evolution optimization mechanism. The novel architecture combines quantum feature encoding techniques, deep pattern extraction, and bio-inspired global optimization methods to enhance diagnostic performance, model interpretability, and computational efficiency. QE-DNN serves as the core classification engine of the system that processes the segmented ROIs extracted via Quantum Mask-RCNN. QE-DNN extends quantum convolutional filters and amplitude coding, enabling the model to capture complex and non-linear features such as tumor density variations, irregularity in edges, and intensity textures from CT-DICOM images. Figure 5 shows the clear architecture model of the proposed QEDNN-AFDE model and how it detects and classifies tumor in various stages. The key characteristics of the QE-DNN model are,

1. Amplitude encoding of inputs - Compress HD pixel values into Quantum probability amplitudes
2. Quantum Convolutional Layers - Inspired by quantum gates and learns spatial deep features
3. Multi-Output Classification - Performs multiple tasks simultaneously to attain target classes
4. Quantum Inspired Activation - Simulates superposition-like behavior using PAF (Parametric Activation Function)

After the process of Quantum amplitude encoding and Convolutional feature mapping which is shown in the previous sections, quantum parametric activation is done to enable smooth transition between activated and inactivated quantum states which is modelled as,

$$Q(Act)(z) = \frac{1}{1+e^{-\alpha z}} + \gamma \cdot \tanh(\beta z) \quad \dots(7)$$

where, α, β, γ are the adaptive parameters which controls the non-linear and simulating super position activation function. In order to activate multi-class total loss function, binary and categorical cross-entropy is combined and expressed in the below equation 8.

$$L_{QEDNN} = \gamma_1 \cdot L_{bin} + \gamma_2 \cdot L_{cat} \quad \dots(8)$$

where, γ_1 and γ_2 balances the tumor detection and classification objectives during the implementation process.

To overcome convergence delays and sub-optimal training in high dimensional deep neural networks, the ADFE mechanism is integrated to optimize the hyperparameter of QE-DNN. AFDE is a bio-inspired optimizer combining firefly exploratory movements with mutation and crossover strategies of Differential Evolution. This dual strategy improves diversity and fine-tuning (Exploration and Exploitation) during training in different iterations/epochs.

In AFDE, firefly movement modeling is the starting phase where fireflies are distributed in the search space, each represents a candidate solution. A firefly i moves towards a better (brighter) firefly j based on perceived attractiveness. The firefly attraction movement is expressed mathematically in equation 9.

$$x_i^{t+1} = x_i^{(t)} + \beta_0 e^{-\gamma \|x_i^{(t)} - x_j^{(t)}\|^2} (x_j^{(t)} - x_i^{(t)} + \alpha \cdot \epsilon_i) \quad \dots(9)$$

where, β_0 denotes initial attractiveness, γ is light absorption coefficient and α is the randomization factor. Here, mutation and crossover take place using DE-based mutation to improve local search. The mutation vector v_i is expressed as,

$$v_i = x_{r1} + F \cdot (x_{r2} - x_{r3}) \quad \dots(10)$$

where, x_{r1}, x_{r2}, x_{r3} are randomly selected candidate solutions and F denotes the scaling factor.

Table 1. Literature Analysis of Specific State-of-Art Models

Name of the Authors & Model	Methods Adapted	Merits	Demerits	Limitations of Lung Cancer Detection Multi-Class Classification
Wei et.al ¹¹ has done Quantum CNN Survey	Quantum Machine Learning based convolutional layers	Employment quantum methods for imaging	Lacks optimization and deep segmentation	No hyperparameter tuning for better optimization accuracy
Nithyanandh et.al ¹² proposed EAB-IFPA	Improved Firefly bio-inspired optimization	Deep optimization and hyper parameter tuning process Highlights early detection	Limited to specific number of datasets	Doesn't address medical image diagnosis for complex datasets
Ahmad and Alqurashi ¹³ introduced DL Cancer Detection	Deep learning models with image processing		It is Conceptual and lacks CT data trials	Lacks empirical medical tests and convergence
Bharathi and Shalimi ¹⁴ proposed Hybrid Attention + Heuristic DL method	Attention + Heuristic DL method	Strong attention mechanism focuses on specific tumor zones	Lacks generalizability beyond fusion	Not suitable for real-time diagnostics
Jaiganesh and Nithyanandh ¹⁵ utilized Virus Swarm algorithm	Virus Swarm Bio-Inspired	Effective optimization	Not suitable for real-world application	Doesn't work for complex 2D and 3D datasets
Elhassan et.al ¹⁶ developed Dual-Model DL	CNN + Classifier Fusion	Fusion improves classification	Binary classification only	No stage detection support
Choudhury et.al ¹⁷ introduced TL-Based CT Detection	Transfer Learning with CNN approach	Efficient CT-based transfer accuracy	No dynamic segmentation layer	Limited generalizability
Nithyanandh and Jaiganesh ¹⁸ employed ABC-based ML model	ABC Bio-Inspired algorithm	Fast search process locally and globally	No clinical trials were done	More focus on text datasets
Sharma et.al ¹⁹ proposed Lung-Colon DL	Deep CNN Models	High performance for multi-cancer	No severity grading	Fails on overlapping lesions
Arularasan et.al ²⁰ proposed DL Image Recognition	Deep Learning Feature Recognition	Boosts SLR accuracy	No multi-class adaptability	Computational complexity and limited feature analysis
Devi et.al ²¹ introduced GANs + Bio-Inspired Model	GANs based deep learning model	Robust mechanism to reduce data loss	No clinical image validation	Lacks on severity grading and multi-class analysis
Abe et.al ²² utilized Robust DL CT	Enhanced CNN from CT images	Handles varied CT image quality	No optimization layer	No dual-task output
Crasta et.al ²³ developed Novel DL CT Arch Model	Custom CNN + Feature Maps	Custom-tailored for tumor zones	No quantum features	No use of quantum-inspired design
Prabhu et.al ²⁴ proposed	Virus Swarm Bio-Inspired	Adaptive to network	Dynamic pre-processing	Local and Global feature

Bio Swarm Routing	changes	analysis
Hroub et.al. ²⁵ used Explainable DL	Justified predictions via explainability	No severity score predicted
Selvam and Joy ²⁶ employed AEN + Mask-RCNN	Effective plant segmentation technique adapted	Different dataset domain
Nithyanandh ²⁷	Real-time object identification	Lacks severity analysis
YOLOv8 + CNN	Improves learning with missing data	Lacks label completion tools
Gao et.al. ²⁸ introduced DL Annotation	Efficient dual-path inference	Needs label completion tools
Li et.al. ²⁹ utilized Dual Stream HNN	Predicts feature for allergies	Not suitable for DICOM imaging
Kwon et.al. ³⁰ proposed model for Epitope Prediction		Deep segmentation and binary classification
Explainable CNNs		Lacks segmentation
Autoencoder + Mask-RCNN		Non-lung domain
YOLOv8, Deep CNN		Focused on object tasks only
Robust DL + Incomplete Labels		Limited to partial labels
Hybrid Neural Network		No explainability module
Epitope Deep Learning Classifier		Image analysis is limited

The crossover step generates offspring from parent and mutant vector. The Differential Evolution binomial crossover is represented as,

$$U_{i,j} = \begin{cases} U_{i,j} & \text{if } rand_j \leq C_r \text{ or } j = j_{rand} \\ X_{i,j} & \end{cases} \dots(11)$$

where, C_r is crossover rate and J_{rand} denotes gene selection from the mutant. Finally, fitness evaluation takes place using the fitness function,

$$f(x) = -L_{QEDNN}(x) \dots(12)$$

where, offspring with better fitness replace their parents and ensures progressive convergence towards optimal hyper-parameter tuning process. The integrated learning workflow of hybrid QEDNN-AFDE framework operates in iterative training cycles. In every iteration the following steps will be executed and cycled.

1. ROIs from Q-Mask-CNN will be the input to QEDNN
2. Amplitude Encoding transforms input to quantum mechanisms
3. QEDNN processes data using quantum layers
4. AFDE evaluates QEDNN's performance and updates the learning rates, dropout rates and weights
5. Training continues until convergence met based on scores.

The major advantage of using quantum framework is, i) precision learning ii) adaptive tuning, iii) multi-class output capability and iv) generalizability. Also, the model's ability clearly shows that it is highly fit to work on real-time data to detect and classify the lung tumors as a part of initial screening process in healthcare sector.

Iterative Training and Optimization Strategy

The hybrid QEDNN-AFDE framework is trained using a dynamic, iterative strategy to refine the quantum model's accuracy, stability, and generalization. This iterative approach integrates a multi-modal bio-inspired feedback-based optimization to adaptively tune hyperparameters, layer-wise configurations, and classification thresholds across multiple learning cycles. In QEDNN, each iteration is an evolutionary step

Table 2. Dataset Description & Features

Attributes	Values
Total Number of Datasets	251135
Number of Training Data	175794
Number of Testing Data	50227
Number of Validating Data	25114
Number of Major Features	20

Number of Major Features Extracted

Image_ID, Pixel_Intensity_Distribution, Texture_Entropy, Nodule_Size, Shape_Descriptors, Lung_Lobe_Location, Bounding_Box_Coordinates, Gray_Level_Co-occurrence_Matrix (GLCM), Histogram_Equalization_Values, Wavelet_Coefficients, Segmentation_Mask_Accuracy, Edge_Sharpness_Index, Mean_Intensity, Standard_Deviation, Skewness, Kurtosis, Gradient_Orientation, Quantum_Encoded_Feature_Vector
 Class_Label (0: Healthy, 1: Cancer, 2: Severity)

in which the model evolves better to discriminate healthy tissues, malignant nodules, and their severity scores. In every training epoch, iteration-based data feeding is done, where batches of segmented ROI patches are sent as input to QEDNN. Each ROI represents target classes 0, 1, and 2 and includes spatial features such as edge sharpness, texture gradients, and gray-level distribution. At the end of each epoch, AFDE is invoked to evaluate the current QEDNN performance based on the fitness score of candidates. AFDE generates multiple candidate solutions that represent different learning rates and dropout rates. The candidate yields the lowest classification loss, and a high segmentation overlap is selected for the next iteration.

Confusion Matrix and True Value Prediction

A 3x3 confusion matrix is performed to predict the actual values of three target classes: healthy, cancer, and severity score analysis. It is observed that the proposed QEDNN-AFDE model indicates high accuracy and less misclassification

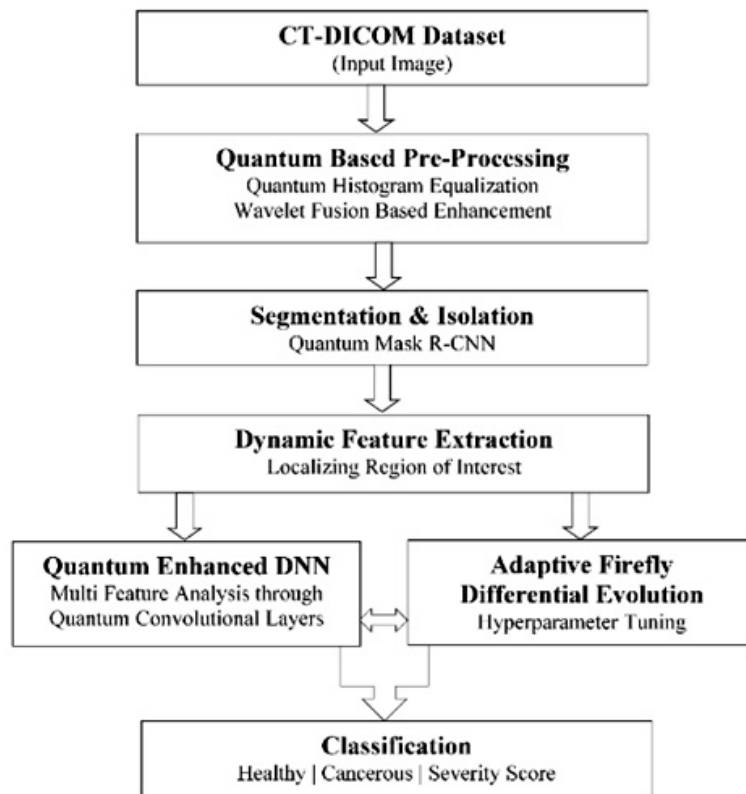


Fig. 1. Flow Diagram of the Proposed Model

during internal training with a 70% ratio of data. During testing, the model maintains high consistency and retains the discriminative power between overlapping categories such as cancer vs

severity. During validation, unbiased tuning and consistent precision are tested to predict the false rates and stability of the model to deploy in a real-world clinical decision support system. The model

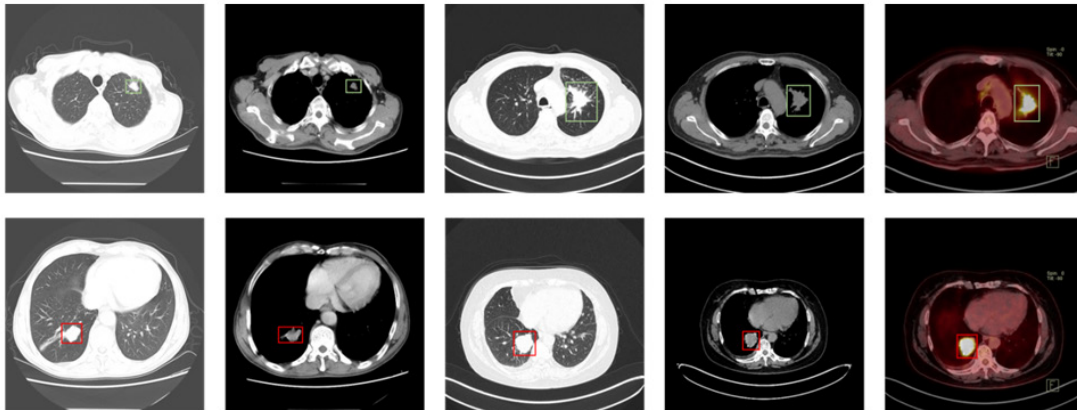


Fig. 2. Lung CT-DICOM Annotated Image.³¹

Image Source (<https://www.cancerimagingarchive.net/collection/lung-pet-ct-dx/>)

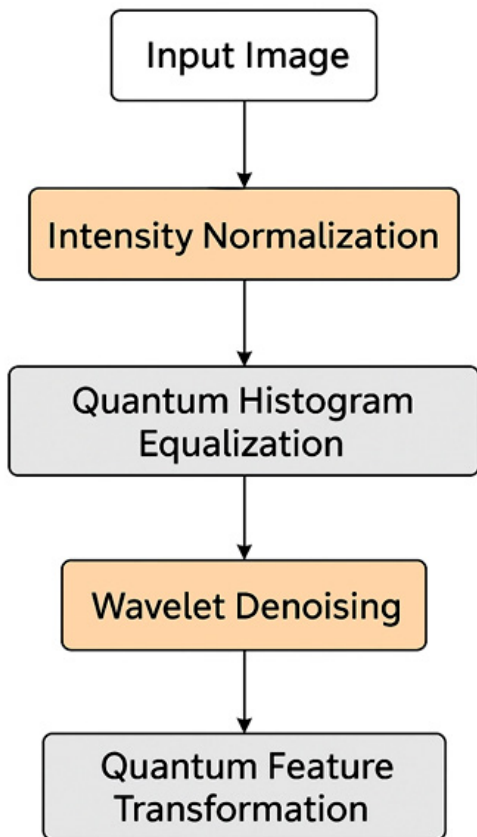


Fig. 3. Pre-Processing of CT-DICOM Images

reflects consistent precision during validation. The proposed QEDNN-AFDE provides high model learning consistency and class separation in the training and testing phase with reliable tuning performance. It shows low variance with realistic deployment readiness.

RESULTS

The performance evaluation of the proposed QEDNN-AFDE is done using the MATLAB simulation tool to validate the accuracy, generalization, and diagnostic reliability in detecting and classifying the tumors from CT-DICOM images. A 3x3 confusion matrix is performed across multiple iterations to capture three target classes (Healthy (0), Cancer Detected (1), and Severity Level (2)) and truth values. Seven performance evaluation metrics are used, which help reinforce the proposed model's ability as one of the high-precision diagnostic tools highly suitable for dynamic integration into clinical decision support systems. The equations 13-20 mentioned below are used to calculate the ratio of actual outcomes of each metric across several iterations is shown in the discussions section.

The results of the comparative models are shown and discussed technically in this section.

The findings show the robust detection and classification of the QEDNN-AFDE model against existing models such as SVM-WSS7, GCPSONN8, 3D-DLCNN9, and ECNNDE-BCE10. The MATLAB graph of all the metrics shows the output values where the X-axis denotes models, and the Y-axis denotes percentages. Figure 7-12 indicates the performance evaluation metrics and discussions on how the model reflects effective detection and classification of lung tumors under various iterations. The new model outperforms all the existing models across all metrics and iterations. Various epochs with different batch sizes are carried out to get desired output values.

$$Accuracy = \frac{(TPR+TNR)}{(TPR+TNR+FPR+FNR)} \times 100 \quad \dots(13)$$

$$Sensitivity = \frac{TPR}{(TPR+FNR)} \times 100 \quad \dots(14)$$

$$Specificity = \frac{TNR}{(TNR+FPR)} \times 100 \quad \dots(15)$$

$$Dice\ Coefficient = \frac{2*TP}{(2*TP+FPR+FNR)} \times 100 \quad \dots(16)$$

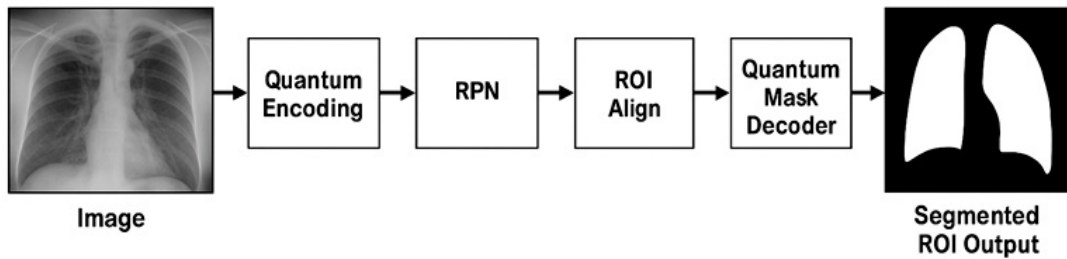


Fig. 4. Quantum Mask R-CNN Segmentation

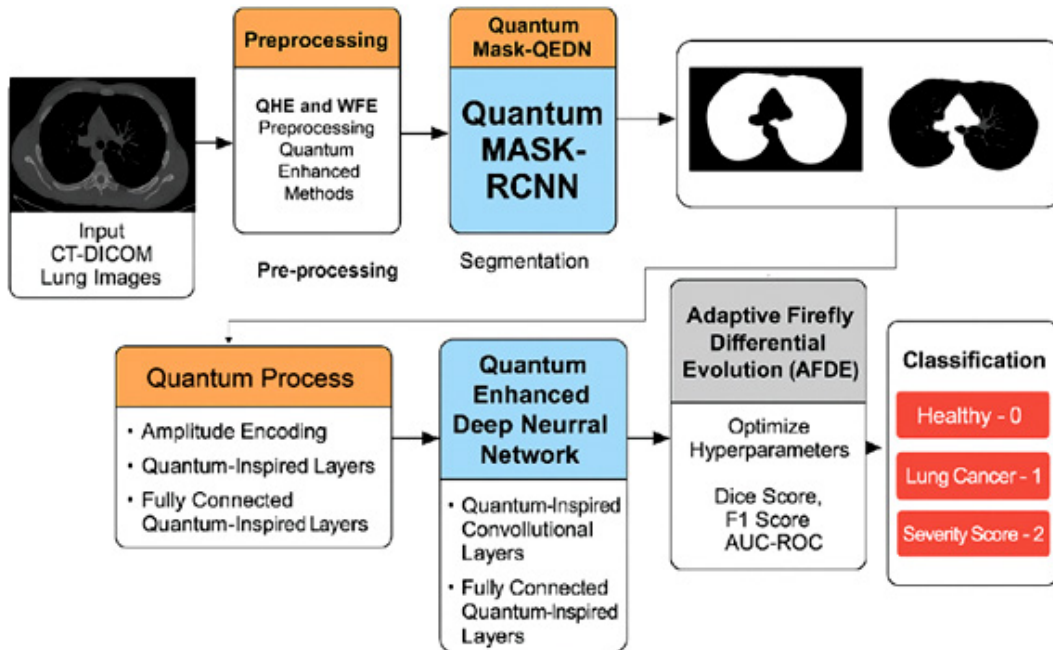


Fig. 5. QEDNN-AFDE Architecture

$$AUC - ROC (TP \& FP) \quad TP = \frac{TPR}{(TPR+FNR)}, FP = \frac{FPR}{(FPR+TNR)} \quad \dots(17)$$

$$Logirathmic \ Loss = -\frac{1}{N} \sum_{i=1}^N (y_i \log(p_i) + (1 - y_i) \log(1 - p_i)) \quad \dots(18)$$

$$F1Score = \frac{2 * (Precision * Recall)}{(Precision + Recall)} \quad \dots(19)$$

$$MCC = \frac{T_1}{\sqrt{T_2 * T_3 * T_4 * T_5}} \times 100 \quad \dots(20)$$

where, MCC denotes Matthews Correlation Coefficient and the true values are derived by the equation, T1 = (TPR×TNR-FPR×FNR), T2 = (TPR+FPR), T3 = (TPR+FNR), T4 = (TNR+FPR), and T5 = (TNR+FNR).

• Sensitivity and Specificity: Measures the model’s ability to accurately detect actual cancer and non-cancerous cases. High sensitivity ensures that malignant cases are not missed, and high specificity ensures that no healthy individuals are wrongly

diagnosed.

• Accuracy: The overall correctness of predictions by calculating the ratio of positive and negative against total samples. This metric validates the target classes and their outcomes.

• AUC-ROC: The metric quantifies the model’s ability to distinguish the TPR, FPR, and FNR between target classes. Higher AUC indicates better discriminative performance in robustly separating the classes.

• Log Loss: The confidence levels are measured, and the predicted probability distribution is checked to see how close it is to the actual label. Lower log loss ensures that the outputs are trustworthy for clinical use.

• Dice Coefficient: Spatial overlap metric, especially for segmentation tasks, compares predicted region and ground truth and assesses how accurately the lung nodules are localized.

• F1 Score: It balances the FPR and FNR and offers more accuracy in imbalanced datasets with minimal trade-offs.

DISCUSSIONS

Sensitivity and Specificity Comparative Analysis

The sensitivity and specificity analysis of the proposed quantum-based bio-inspired

Table 3. Sample iteration values of three target classes

	Confusion Matrix	Correct Healthy Predictions	Correct Cancer Predictions	Correct Severity Predictions
Training		12,100	16,750	15,540
Testing		4,100	5,700	4,980
Validation		2,050	2,825	2,495

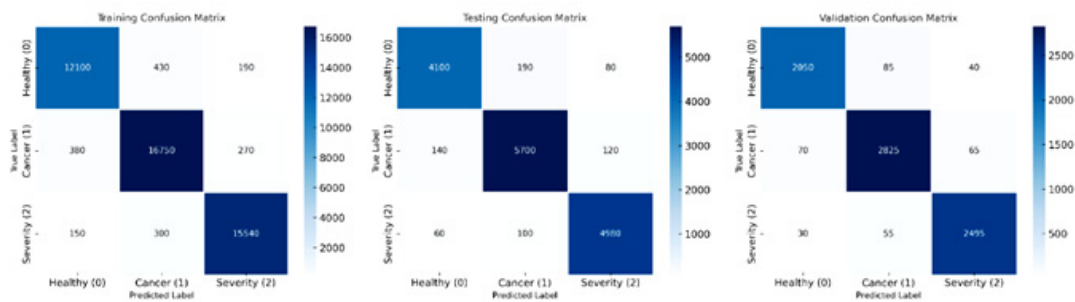


Fig. 6. 3x3 Confusion Matrix of Sample Iterations

Quantum Based Bio-Inspired Detection and Classification Process Steps (QEDNN-AFDE)

1. **Input:** CT-DICOM lung cancer image dataset from TCIA repository
2. **Begin:** Load the dataset $DICOM\ dataset = load(dicom_data.mat)$
3. **Initial Pre-Processing:** Convert all images to grayscale with resolution normalization (512×512 pixels).
4. Perform intensity normalization using $min - max\ scaling$ for pixel value consistency.
5. Apply QHE to enhance contrast and boundary differentiation.
6. Implement $wavelet\ fusion$ to suppress background noise while preserving tumor edges.
7. Perform $amplitude\ encoding$ to map pixel intensity vectors into Q_{states} .
8. Store Q_{images} for feature-enhanced processing.
9. Load bounding box annotations and labels $Healthy - 0, Cancer\ 1, Severity - 2$
10. Apply Q_{MASK}_{RCNN} to detect and segment lung nodules.
11. Generate segmentation masks to extract Q_{ROI} from each image.
12. Label each Q_{ROI} with its corresponding class and assign to training, testing, validation subsets.
13. Initialize $QEDNN_{structure}$ with predefined structure.
14. Pass Q_{ROI} through QEDNN using QC_{layers}
15. Extract multi-dimensional spatial and contextual features from Q_{ROI} .
16. Configure $Layer_{output}$ for binary (tumor detection) and multi-class (severity) classification.
17. Initialize $AFDE_{optimizer}$ for fine-tuning
18. Generate $Population_{initial}$ of fireflies representing QEDNN hyperparameter sets.
19. Compute $Fitness_{score}$ of each firefly using combined loss L_{QEDNN}
20. Update $fireflies$ using firefly movement, mutation, and DE-based crossover operations.
21. Select $Candidate_{solution}$ with minimum loss for next QEDNN $Training_{iteration}$
22. Train QEDNN iteratively over multiple epochs with updated parameters.
23. After each epoch, evaluate model using 3×3 confusion matrix on training, test, validation sets.
24. **Track performance metrics:** Accuracy, Sensitivity, Specificity, F1 Score, Dice Score, AUC-ROC, Log Loss.
25. If performance improvement < 0.01% for 5 epochs or Dice > 94% activate early stopping.
26. Store optimal QEDNN-AFDE model parameters for inference.
27. For each test sample, apply segmentation, encode ROI, and classify using trained model.
28. **Output classification:** Healthy (0), Tumor Detected (1), or Severity Score (2 – mild/moderate/severe).
29. Visualize results with mask overlays, confusion matrices, and metric summaries.
30. End

QEDNN-AFDE model shown in Figure 7, achieved an exceptional diagnostic performance of 95.2% and 95.8%, reflecting the strength in detecting actual tumor cases by excluding healthy instances. The quantum pre-processed masks ensure accurate region extraction in this model, improving classification boundaries. The quantum-enhanced convolutional layers preserve subtle diagnostic features, and AFDE fine-tunes the hyperparameters to optimize recall and precision simultaneously. QEDNN-AFDE consistently discriminates against cancer and health across varying nodule shapes and densities, helping the model be suitable for deployment in real-time scenarios for cancer screening and severity score analysis in the healthcare sector.

Accuracy Comparative Analysis

Figure 8 shows the overall accuracy of the proposed QEDNN-AFDE model, which attains 96.4%, confirming its ability to identify and classify the target classes such as cancer,

healthy, and severity scores with the help of DICOM image datasets. QEDNN overcomes the limitations of existing models and allows deep extraction and multi-level spatial feature extraction from CT-DICOM images. The AFDE fine-tunes the learning parameters dynamically to ensure deep convergence towards optimal weights across various iterations, which helps to minimize FPR and FNR. The high accuracy of this QEDNN-AFDE reflects the model’s suitability in multi-class environments, which improves the generalization without compromising the diagnostic precision, making the system trustworthy for dynamic integration in clinical decision-support pipelines.

AUC-ROC Analysis

The performance analysis of the AUC-ROC metric is showcased in Figure 9. This metric serves as a robust discriminative evaluation across all target classes. The QEDNN-AFDE exhibits 0.98 AUC, indicating the ability to classify healthy, cancerous, and severity-score lung images. The

Table 4. Sensitivity and Specificity Analysis

Metrics / Schemes	SVM-WSS ⁷	GCPSO-PNN ⁸	3D-DLCNN ⁹	ECNN-BCE ¹⁰	QEDNN-AFDE (Proposed)
Sensitivity	76.52	81.78	86.35	93.81	95.20
Specificity	78.65	83.40	88.48	94.52	95.80

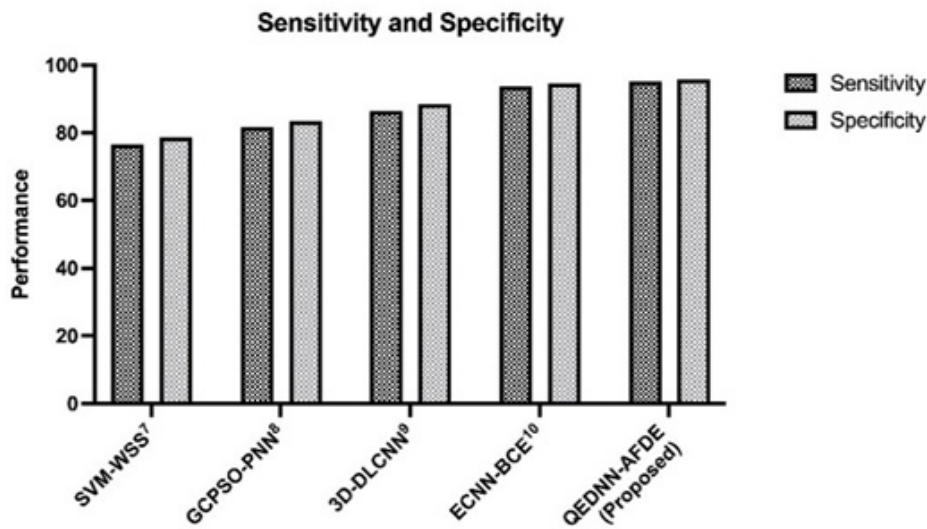


Fig. 7. Sensitivity and Specificity Graph

higher AUC denotes that the hybrid architecture is tuned ideally based on thresholds. The quantum encoding mechanism allows the preservation of high dimensional texture cues while AFDE adjusts the classification boundaries for each class. This dual method resulted in distinct score distributions, making them more evident in ROC space. The multi-class ROC analysis consistently shows

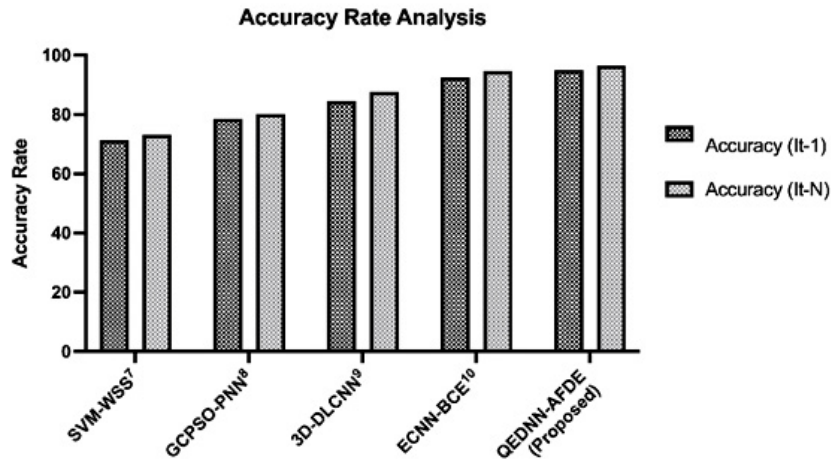


Fig. 8. Accuracy Analysis Graph

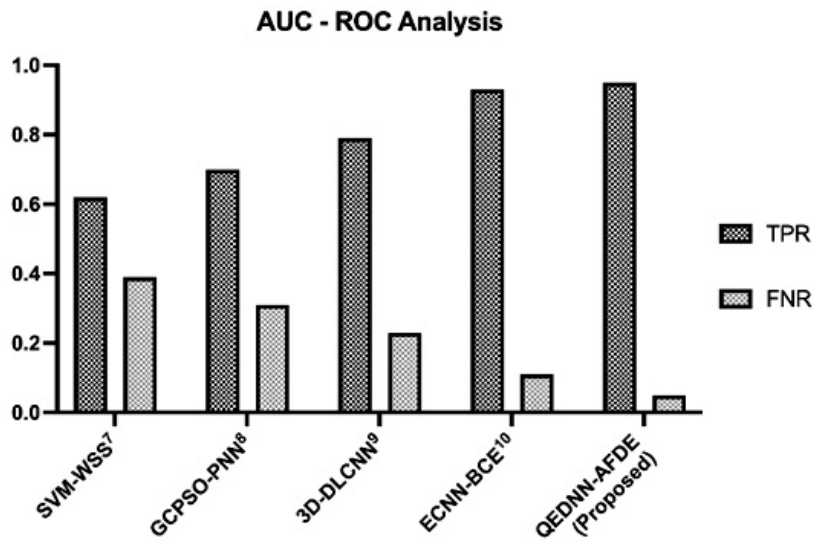


Fig. 9. AUC-ROC Analysis Curve

Table 5. Accuracy Rate Analysis

Metrics / Schemes	SVM-WSS ⁷	GCP SO-PNN ⁸	3D-DL CNN ⁹	ECNN-BCE ¹⁰	QEDNN-AFDE (Proposed)
Accuracy (It-1)	71.26	78.48	84.52	92.45	94.91
Accuracy (It-N)	73.18	80.08	87.68	94.73	96.40

high TPR and FPR across all categories, which is scalable for diverse lung pathology datasets. The results of the proposed QEDNN-AFDE model are compared against existing models SVM-WSS⁷, GCP SO-PNN⁸, 3D-DLCNN⁹, and ECNNDE-BCE¹⁰. The promising results show that QEDNN-AFDE outperforms the existing models with high discrimination power in accurate classification and smooth diagnosis capability.

Dice Coefficient Analysis

The comparative result analysis of the dice coefficient metric is shown in Figure 10. This metric is a spatial overlap to evaluate the segmentation quality. The proposed QEDNN-AFDE achieved a dice score of 94.6%, demonstrating its ability to localize and segment the lung nodules in CT-

DICOM images accurately. This was achieved by quantum Mask-RCNN, which enhanced the ROI boundaries through quantum-assisted attention mechanisms. QHE and WEF ensure edge preservation to improve ROI mask clarity and alignment with actual nodular structures. QEDNN-AFDE identifies irregular shapes, small tumors, and overlapping anatomical structures in the DICOM dataset. The model minimized FNR within nodules and reduced false positive markings outside the target areas. The consistent results with high-overlap segmentation output are validated across multiple epochs and iterations. This model helps in pre-treatment planning, surgical mapping, and tumor progression analysis.

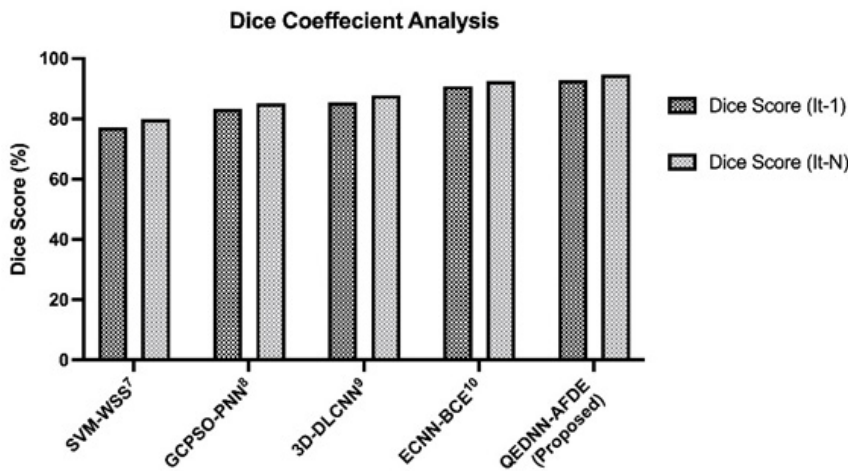


Fig. 10. Dice Coefficient Graph

Table 6. AUC-ROC Analysis

Metrics / Schemes	SVM-WSS ⁷	GCP SO-PNN ⁸	3D-DLCNN ⁹	ECNN-BCE ¹⁰	QEDNN-AFDE (Proposed)
TPR	0.62	0.70	0.79	0.93	0.95
FNR	0.39	0.31	0.23	0.11	0.05

Table 7. Dice Coefficient Analysis

Metrics / Schemes	SVM-WSS ⁷	GCP SO-PNN ⁸	3D-DLCNN ⁹	ECNN-BCE ¹⁰	QEDNN-AFDE (Proposed)
Dice Score (It-1)	77.19	83.17	85.45	90.78	92.81%
Dice Score (It-N)	79.80	85.16	87.76	92.44	94.60%

Logarithmic Log Analysis

A comparative analysis of the logarithmic loss of different models is shown in Figure 11. It evaluates the confidence of probability-based predictions, where lower values indicate fewer errors. The proposed QEDNN-AFDE achieved low log loss due to a robust probabilistic learning design. As QDNN uses the parameter shift rule, the prediction probabilities are maximized in all iterations. This strategy is mainly used in borderline cases, where overconfident misclassification scores are standard in deep neural networks. The low log loss validates the ability of the proposed quantum-based model to generate reliable confidence scores,

which are essential for clinical decision-making, especially in automated reported systems to assess diagnostic risk.

F1-Score Comparative Analysis

Figure 12 shows the harmonic mean analysis called F1 Score of the proposed QEDNN-AFDE to evaluate underclass imbalance, which is common in clinical datasets. The proposed work shows a remarkable 95.2% F1 score, which signifies its balanced performance in detecting TPR and avoiding False rates. The hybrid quantum convolutional layers extracted spatial-temporal features that preserved essential tumor patterns in low-contrast regions. This dynamic

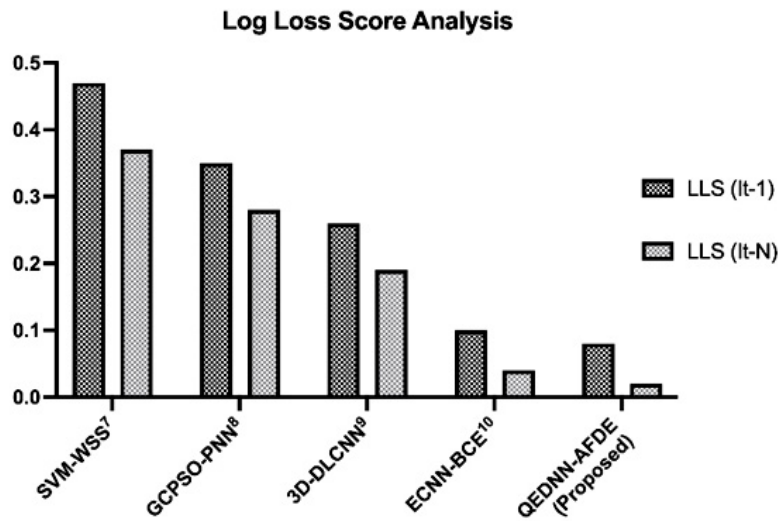


Fig. 11. Log Loss Graph

Table 8. Log Loss Score Analysis

Metrics / Schemes	SVM-WSS ⁷	GCPPO-PNN ⁸	3D-DLNN ⁹	ECNN-BCE ¹⁰	QEDNN-AFDE (Proposed)
LLS (It-1)	0.47	0.35	0.26	0.10	0.08
LLS (It-N)	0.37	0.28	0.19	0.04	0.02

Table 9. Analysis of F-Score

Metrics / Schemes	SVM-WSS ⁷	GCPPO-PNN ⁸	3D-DLNN ⁹	ECNN-BCE ¹⁰	QEDNN-AFDE (Proposed)
F1 Score (It-1)	75.35	80.68	86.55	91.30	93.74
F1 Score (It-N)	78.18	82.74	88.76	93.42	95.20

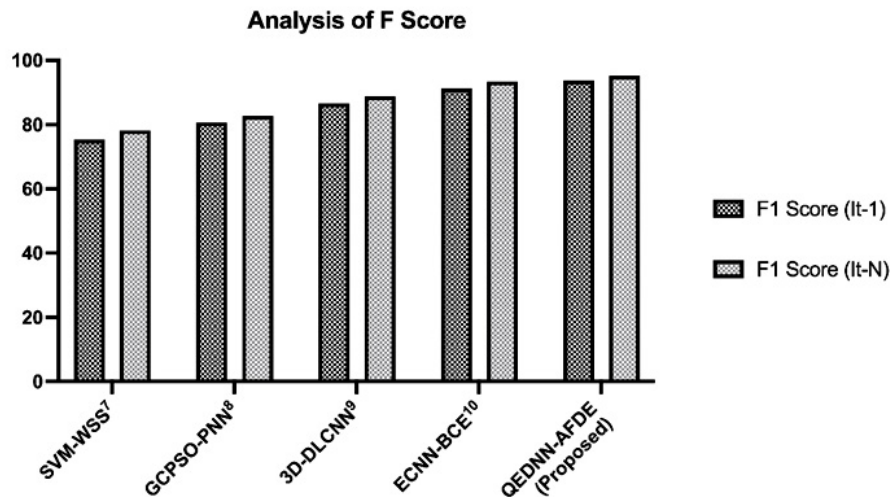


Fig. 12. F1 Score Analysis Graph

learning strategy allows the proposed QEDNN-AFDE model to maintain high performance and consistency across all three target classes. A high F1 score reflects the diagnostic fidelity of the quantum model and highlights the capability to generalize input conditions and imaging variations across many patients. This will act as a pre-requisite for AI-based real-time deployment in radiology workflows.

Merits & Demerits of the Proposed Technique

The proposed QEDNN-AFDE model significantly outperforms baseline models such as SVM-WSS, GCPPO-PNN, 3D-DLNN, and ECNN-BCE by utilizing the quantum-inspired feature encoding and adaptive swarm-based hyperparameter optimization. The key merits include enhanced convergence speed, superior sensitivity and specificity, and improved generalization across varying clinical CT-DICOM large-scale datasets. Unlike baseline optimization models, QEDNN-AFDE effectively minimizes overfitting through dynamic search capabilities. However, the computational complexity of QEDNN and the resource overhead introduced by AFDE may pose challenges in low-resource environments. Additionally, integration of QAE requires more careful calibration compared to conventional CNN layers. Despite these constraints, the method demonstrates considerable promise in early lung cancer detection which offers

interpretability, scalability, and accuracy gains over prevailing techniques.

CONCLUSION

This proposed QEDNN-AFDE research work presents a dynamic integration of quantum deep learning and bio-inspired optimization to address the limitations of lung tumor detection and severity analysis from CT-DICOM images. QE-DNN and Q-CNN stand robust foundation of the model, successfully operates synergistically to detect healthy and cancerous tissues with tumor severity scores. Advanced pre-processing techniques such as histogram equalization and wavelet fusion ensure structural clarity analysis across complex features of DICOM. The bio-inspired AFDE algorithm improves the hyperparameter significantly, leading to a well-regularized and high-performing model across diverse patient image variations. The outperforming results with 96.4% accuracy, 95.2% sensitivity, 95.8% specificity, 95.2% F1 score, 94.6% dice coefficient, 0.02 Log Loss and AUC-ROC with 0.95 TPR, and 0.05 FNR highlights the model's potential for early and accurate diagnosis, prognosis planning and decision support in oncology workflows. The study elevates the diagnostic capabilities of deep-learning integration in radiology and demonstrates

the feasibility of a quantum-inspired framework for real-world medical applications. By merging advanced computational methods with biologically motivated learning strategies, QEDNN-AFDE establishes a new benchmark in precision image analysis.

Though the model achieves outstanding performance, the implementation is limited to quantum simulators rather than actual quantum hardware. Also, real-time deployment in clinical environments requires validation under imaging protocols and multi-institutional datasets to ensure the model's robustness.

ACKNOWLEDGEMENT

The authors would like to express their sincere gratitude to their respective institutions, PKR Arts College for Women, Gobichettipalayam, Tamil Nadu and PPG College of Arts & Science, Affiliated to Bharathiar University, Coimbatore, Tamilnadu, India for their support throughout this research.

Funding Sources

The author(s) received no financial support for the research, authorship, and/or publication of this article.

Conflict of interest

The authors do not have any conflict of interest.

Data Availability Statement

This statement does not apply to this article. Simulation data will be provided on request.

Ethics Statement

This research did not involve human participants, animal subjects, or any material that requires ethical approval.

Informed Consent Statement

This study did not involve human participants, and therefore, informed consent was not required.

Clinical Trial Registration

This research does not involve any clinical trials, only software simulations are carried out.

Author Contribution

Each author has significantly contributed to this research; Kalaivani Devaraj has collected the data and identified problem statement and objectives as an initial phase. Also, the complete methodology part is done by her with all implementation using

simulation tools and played a key role in refining the manuscript as a corresponding author; Dheepa Ganapathy has done a thorough paper evaluation, language check, supervision and guidance for implementation as a co-author and supervisor and made all the editorial checks, paper revision etc. Both the authors have given their approval for its publication.

REFERENCES

1. Zia UrRehman, Yan Qiang, Rukhma Aftab & Juanjuan Zhao. Effective lung nodule detection using deep CNN with dual attention mechanisms. *Scientific Reports*. 2024;14(1). DOI: <https://doi.org/10.1038/s41598-024-51833-x>
2. Martis JE, M S S, R B, Mutawa AM, Murugappan M. Novel Hybrid Quantum Architecture-Based Lung Cancer Detection Using Chest Radiograph and Computerized Tomography Images. *Bioengineering*. 2024; 11(8):799. <https://doi.org/10.3390/bioengineering11080799>
3. V. R. N, Chandra S. S. V. ExtRanFS: An Automated Lung Cancer Malignancy Detection System Using Extremely Randomized Feature Selector. *Diagnostics*. 2023; 13(13):2206. <https://doi.org/10.3390/diagnostics13132206>
4. Wahab Sait AR. Lung Cancer Detection Model Using Deep Learning Technique. *Applied Sciences*. 2023; 13(22):12510. <https://doi.org/10.3390/app132212510>
5. Klangbunrueang R, Pookduang P, Chansanam W, Lunrasri T. AI-Powered Lung Cancer Detection: Assessing VGG16 and CNN Architectures for CT Scan Image Classification. *Informatics*. 2025; 12(1):18. <https://doi.org/10.3390/informatics12010018>
6. S Nithyanandh and V Jaiganesh. Quality of service enabled intelligent water drop algorithm based routing protocol for dynamic link failure detection in wireless sensor network. *Indian Journal of Science and Technology*. 2020;13(16):1641-1647. <https://doi.org/10.17485/ijst/v13i16.19>
7. Chaturvedi P, Jhamb A, Vanani M, Nemade V. Prediction and classification of lung cancer using machine learning techniques. *IOP Conference Series Materials Science and Engineering*. 2021;1099(1):012059. <https://doi.org/10.1088/1757-899x/1099/1/012059>
8. Jagadeesh K, Rajendran A. Improved model for Genetic Algorithm-Based Accurate lung cancer segmentation and classification. *Computer Systems Science and Engineering*. 2022;45(2):2017-2032. <https://doi.org/10.32604/csse.2023.029169>

9. Eldho KJ, Nithyanandh S. Lung Cancer Detection and Severity Analysis with a 3D Deep Learning CNN Model Using CT-DICOM Clinical Dataset. *Indian Journal of Science and Technology*. 2024;17(10):899-910. <https://doi.org/10.17485/ijst/v17i10.3085>
10. Kalaivani D, Dheepa G. Deep Learning Enhanced CNN with Bio-Inspired Techniques and BCE For Effective Lung Nodules Detection & Classification For Accurate Diagnosis. *Indian Journal of Science and Technology*. 2024;17(37):3851-3864. <https://doi.org/10.17485/ijst/v17i37.2649>
11. Wei L, Liu H, Xu J, et al. Quantum machine learning in medical image analysis: A survey. *Neurocomputing*. 2023;525:42-53. <https://doi.org/10.1016/j.neucom.2023.01.049>
12. Nithyanandh S, Omprakash S, Megala D, Karthikeyan MP. Energy Aware Adaptive Sleep Scheduling and Secured Data Transmission Protocol to enhance QoS in IoT Networks using Improved Firefly Bio-Inspired Algorithm (EAP-IFBA). *Indian Journal of Science and Technology*. 2023;16(34):2753-2766. <https://doi.org/10.17485/ijst/v16i34.1706>
13. Ahmad I, Alqurashi F. Early cancer detection using deep learning and medical imaging: A survey. *Critical Reviews in Oncology/Hematology*. 2024;204:104528. <https://doi.org/10.1016/j.critrevonc.2024.104528>
14. Bharathi PS, Shalini C. Advanced hybrid attention-based deep learning network with heuristic algorithm for adaptive CT and PET image fusion in lung cancer detection. *Medical Engineering & Physics*. 2024;126:104138. <https://doi.org/10.1016/j.medengphy.2024.104138>
15. S Nithyanandh and V Jaiganesh. Dynamic Link Failure Detection using Robust Virus Swarm Routing Protocol in Wireless Sensor Network. *International Journal of Recent Technology and Engineering (IJRTE)*. 2019;8(2):1574-1579. <https://doi.org/10.35940/ijrte.b2271.078219>
16. Elhassan SM, Darwish SM, Elkaffas SM. An enhanced lung cancer detection approach using Dual-Model Deep Learning technique. *Computer Modeling in Engineering & Sciences*. 2024;0(0):1-10. <https://doi.org/10.32604/cmcs.2024.058770>
17. Choudhury AR, Rautray J, Mishra P, Kandpal M, Dalai SS. Deep Learning Based Automated Lung Cancer Detection from CT scan Leveraging Transfer Learning. *Procedia Computer Science*. 2025;258:2748-2759. <https://doi.org/10.1016/j.procs.2025.04.535>
18. Nithyanandh S, Jaiganesh V. Reconnaissance Artificial Bee Colony Routing Protocol to Detect Dynamic Link Failure in Wireless Sensor Network. *International Journal of Scientific & Technology Research*. 2019; 10(10):3244–3251. <https://www.ijstr.org/final-print/oct2019/Reconnaissance-Artificial-Bee-Colony-Routing-Protocol-To-Detect-Dynamic-Link-Failure-In-Wireless-Sensor-Network.pdf>
19. Sharma D, Choubey DK, Thakur K. Lung and Colon Cancer Detection using Deep Learning Techniques. *Procedia Computer Science*. 2025;258:4136-4146. <https://doi.org/10.1016/j.procs.2025.04.664>
20. Arularasan R, Balaji D, Garugu S, Jallepalli V R, Nithyanandh S, Singaram G. Enhancing Sign Language Recognition for Hearing-Impaired Individuals Using Deep Learning. *2024 International Conference on Data Science and Network Security, Tiptur, India*. 2024; 10690989:1-6. <https://doi.org/10.1109/icdsns62112.2024.10690989>
21. Devi PA, Megala D, Paviyasre N, Nithyanandh S. Robust AI Based Bio Inspired Protocol using GANs for Secure and Efficient Data Transmission in IoT to Minimize Data Loss. *Indian Journal of Science and Technology*. 2024;17(35):3609-3622. <https://doi.org/10.17485/ijst/v17i35.2342>
22. Abe AA, Nyathi M, Okunade AA, Pilloy W, Kgoale B, Nyakale N. A Robust Deep Learning Algorithm for Lung Cancer Detection from Computed Tomography Images. *Intelligence-Based Medicine*. January 2025:100203. <https://doi.org/10.1016/j.ibmed.2025.100203>
23. Crasta LJ, Neema R, Pais AR. A novel Deep Learning architecture for lung cancer detection and diagnosis from Computed Tomography image analysis. *Healthcare Analytics*. 2024;5:100316. <https://doi.org/10.1016/j.health.2024.100316>
24. Prabhu TS, Nithyanandh S, Eldho KJ, Karthikeyan B, Vasanthi V. Securing Next Generation 6G Wireless Networks Through Intelligent Bio-Inspired Routing with Energy Optimization for Enhanced Authentication. *Indian Journal of Science and Technology*. 2025;18(23):1882-1895. <https://doi.org/10.17485/ijst/v18i23.850>
25. Hroub NA, Alsannaa AN, Alowaifeer M, Alfarraj M, Okafor E. Explainable deep learning diagnostic system for prediction of lung disease from medical images. *Computers in Biology and Medicine*. 2024;170:108012. <https://doi.org/10.1016/j.compbiomed.2024.108012>
26. Selvam N, Joy EK. Plant Leaf Disease Detection with Multivariable Feature Selection Using Deep Learning AEN and Mask R-CNN in PLANT-DOC Data. *Biosciences Biotechnology Research Asia*. 2024;21(4):1649-1663. <https://doi.org/10.13005/bbra/3333>

27. Dr. Nithyanandh S. Object Detection & Analysis with Deep CNN and Yolov8 in Soft Computing Frameworks. *International Journal of Soft Computing and Engineering*. 2025;14(6):19-27. <https://doi.org/10.35940/ijscce.e3653.14060125>
28. Gao Z, Guo Y, Wang G, et al. Robust deep learning from incomplete annotation for accurate lung nodule detection. *Computers in Biology and Medicine*. 2024;173:108361. <https://doi.org/10.1016/j.combiomed.2024.108361>
29. Li L, Mei Z, Li Y, Yu Y, Liu M. A dual data stream hybrid neural network for classifying pathological images of lung adenocarcinoma. *Computers in Biology and Medicine*. 2024;175:108519. <https://doi.org/10.1016/j.combiomed.2024.108519>
30. Kwon H, Ko S, Ha K, Lee JK, Choi Y. Assessing the predictive ability of computational epitope prediction methods on Fel d 1 and other allergens. *PLoS ONE*. 2024;19(8):e0306254. <https://doi.org/10.1371/journal.pone.0306254>
31. Li P, Wang S, Li T, Lu J, HuangFu Y, & Wang D. A Large-Scale CT and PET/CT Dataset for Lung Cancer Diagnosis (Lung-PET-CT-Dx). *The Cancer Imaging Archive*, 2020. <https://doi.org/10.7937/TCIA.2020.NNC2-0461> (Dataset Collected Source)